ARQII Publication
http://arqiipubl.com/ams
APPLICATIONS OF
MODELLING AND SIMULATION
eISSN 2600-8084
VOL 5, 2021, 66-73

Study of Fluidic Ejection and Nanodroplet Formation

Van Quang Nguyen*, Chung Nguyen Xuan, Dung Hoang Tien, Tung Nguyen Nhu, Hung Pham Tien, Tung Nguyen Tien and Tam Nguyen Chi

Faculty of Mechanical Engineering, Hanoi University of Industry, Viet Nam

*Corresponding author: nguyenvanquang@haui.edu.vn; nguyenquang.kuas@gmail.com

Submitted 21 October 2020, Revised 04 December 2020, Accepted 18 December 2020.

Abstract: Study of fluidic molecule ejection through nozzle diameters of 27.5, 30 and 40 Angstrom (Å) at temperatures of 310, 315 and 333 Kelvin (K) is performed by using the molecular dynamics simulation method. The results show that almost all molecules were ejected out through the nozzle and formed up the fluidic jets on the nozzle's surfaces for all above cases. However, a fluidic jet was not separated out from the nozzle's surface for the case of the 310 K temperature and 27.5 Å diameter under any the pushing force values and ejection time. Otherwise, the jets separate out from the nozzle's surface to produce the fluidic nanodroplets when increasing either the nozzle diameter to 30 Å or the temperature magnitude to 315 K. These demonstrate the nozzle size and temperature magnitude decide to the fluidic ejection and nanodroplet formation.

Keywords: Fluidic ejection, Molecular dynamics simulation; Nanodroplet formation; Nanodroplet separation.

1. INTRODUCTION

This study is carried out due to the interest of reducing the dimension of nano devices while still maintains their stability and function in the printing technology and the electronic and mechanical industrial fields. This research will solve these requirements and predict the results by the molecular dynamic simulation method. The initial design stage for these devices often requires a fast turnaround time of computer models, because it usually involves a massive screening of a large number of design parameters. The fluid dynamics in the nozzle region is described by a flow model. Droplet formation and nozzle fluid dynamics are coupled, and hence solved together, to simulate the inkjet droplet ejection which makes it very useful to explore the large parameter space of inkjet devices in a short amount of time [1].

The model of chemically active particles of a multi-component fluid which focuses on a scenario was leaded to condensation into a liquid droplet. This system displays an interesting and novel behaviors such as oscillations of droplet size and molecular sorting of chemical reactions on the nanoscale [2]. The model of cavity and droplet formation has been observed and explained. The volume of the generated droplet scales with the pore size [3].The process and phenomena of the fluidic ejection though the nozzle have been performed and analyzed by the molecular dynamics simulation. The solution to increases the density of electronic chips for manufacturing the printed circuit board by depositing many nano small thin metal wires on this board [4-5]. Many former researches were revealed to formation and breakup of the fluid nanojets. The dynamics simulations of liquid jet breakup were performed [6]. The molecular dynamics simulation method was used to conduct for liquid droplet formation [7]. Otherwise, the formation of nanodroplets is investigated by the solvent exchanges under the flow conditions. The effects of the flow rate and the flow geometry on the droplet size were discussed [8-10].

The fluidic ejection and jet and nano-droplets formation process have attracted a lot of researches for the design and manufacturing the nano-size devices [11-14]. Finding about influences of the viscosity, wetting and temperature parameters to the fluidic jet and droplet formation was discussed [11, 15-17]. The element of external force which acts to the fluidic ejection is also studied by using the dynamics simulation method. The way for maintaining the fluidic temperature value inside the ejection equipment is highlighted [18-22]. The molecular dynamics simulation method was used to adopt for liquid jet and droplet formations [6, 23]. Nanodroplet formation is a critical process in the development of 3D nano-inkjet printing. A conversion methodology is also adopted to overcome the problem of large coarse-graining factor, which results in unphysical results when the simulation is scaled up to real units. The parameters of the higher temperature and pressure reduce droplet break-up time [7]. The investigations about the experimental process for fluidic ejection were conducted. The effect of the fluidic, nozzle and temperature parameters on the fluidic jet and droplet formation was discussed [24-27].

While that, the almost formally researches have just mainly mentioned to the initial problems of fluidic ejection, the jet formation and breakup for setting up the fluidic droplets. Besides, the problems of fluidic ejection as jet breakup ability to form the nanodroplets, the reasons and evidences for the droplet formation under the effects of the nozzle sizes and temperature values have little been investigated. This research is a development of the previous problem [28] which is used to continue finding about the effect of the various nozzle sizes and temperature values to for the fluidic ejection and jet and droplet

formations under the any pushing force values and ejection time.

2. METHODOLGY

2.1 Simulation Model

Figure 1 shows the simulation model for ejecting the fluidic molecule ejection through the nozzle hole. The back and nozzle plates are composed by gold (Au) atoms and arranged into face-centered cubic (fcc) crystal lattice structures. The back plate is at bottom position of the ejection device which can move vertically in the +*z*-direction when subjected to a pushing force while the nozzle plate is fixed at the above location of the ejection device. The fluidic molecules are the fluidic water which contain inside the ejection device.

The nozzle and back plates have both 5 layers of gold atom with the thickness of each plate is 8.152 Å. A ejection hole is made at the center of the nozzle plate. The water block has the height and width of 60.872 and 101.9 Å, respectively. The periodic boundary conditions are limited for bounding of the ejection device along the *x*-, and *y*-directions of the water block.

2.2 Simulation Scheme

This research performs 5 simulation schemes with three nozzle sizes of 27.5, 30 and 40 Å, three system temperatures of 310, 315 and 333 K and same magnitude of pressing force of 9.0×10^{-10} Newton (N) for all simulation cases as shown in Table 1.

Table 1. Simulation scheme

Case	Nozzle aperture diameter (Å)	Temperature (K)	Pressing force (N)
1	27.5	310	9.0×10^{-10}
2	30	310	9.0×10^{-10}
3	40	310	9.0×10^{-10}
4	27.5	315	9.0×10^{-10}
5	27.5	333	9.0×10^{-10}

2.3 Interaction between Atoms and Molecules

The specific potential model is adopted to estimate the interaction among the atoms H and O of the fluidic molecules. The shifted Lennard-Jones 12-6 potential is used to set up the intermolecular interaction between fluidic molecule and Au atoms. The equilibrium angle of the H-O-H bond is a value of 104.5 degree. The equilibrium length of the H-O bond is a value of 1.0 Å.

The molecular energy function is a sum of the bonding, bending, Van Der Waals and the Coulomb terms [29], which is shown in Equation (1).

$$U = U_{bond} + U_{bend} + U_{vdw} + U_{els}$$

$$= \sum K_b^{OH}(r_i - r_{eq})^2 + \sum K_\theta^{HOH}(\theta_i - \theta_{eq})^2 + \sum [A_{SC}\varepsilon_{ij}\left(\frac{r_0^{ij}}{r_{ij}}\right)^{12} - 2\varepsilon_{ij}\left(\frac{r_0^{ij}}{r_{ij}}\right)^{6} - S_{vdw}(r_{ij})] + \sum [\frac{q^i q^j}{r_{ij}} - S_{els}(r_{ij})], \quad (1)$$

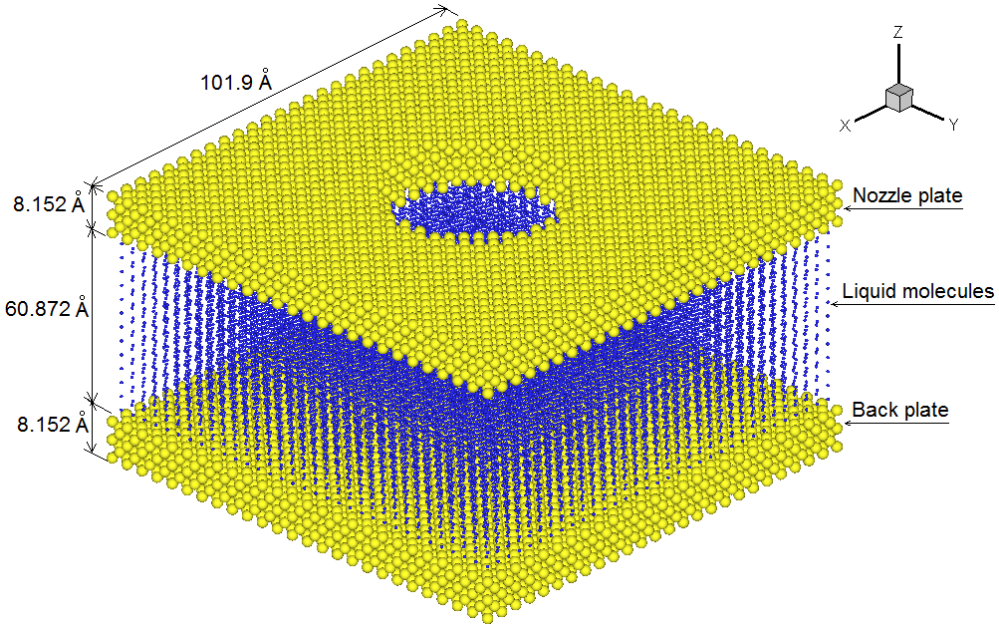

Figure1. Research model

With the truncation shift function of the Van Der Waals force of $S_{vdw}(r_{ij})$ is expressed as in Equation (2).

$$S_{vdw}(r_{ij}) = \begin{cases} U_r - U_{r_c} - (r - r_c)\left(\dfrac{dU}{dr}\right)_{r_c} & \text{for } r < r_c \\ 0 & \text{for } r \geq r_c \end{cases}, \tag{2}$$

and the shift function for the Coulomb's force of $S_{els}(r_{ij})$ is expressed as in Equation (3).

$$S_{els}(r_{ij}) = (r - r_c)\left[\frac{q^i q^j}{r_c^2}\right], \tag{3}$$

The coefficients of $A_{sc}, K_b^{OH}, K_\theta^{OH}, r_i, r_{eq}, \theta_i, \theta_{eq}, r_{ij}$ and r_c are the short distance force, harmonic force constant, angle force constant, O-H bond length, O-H bond equilibrium length, H-O-H bond angle, H-O-H bond equilibrium angle and interatomic and cutoff distances, respectively. O and H have the partial charges q_i and q_j. The interaction between the water molecules and the gold atoms is presented by the SpohHr potential function as shown in Equation (4).

$$U_{Au-H_2O} = U_{Au-O}(r_{Au-O}) + U_{Au-H_1}(r_{Au-H_1}) + U_{Au-H_2}(r_{Au-H_2}), \tag{4}$$

with

$$U_{Au-O}(r) = S_2(r)D_0[\exp(-2\alpha_0(r - r_{e1})) - 2\exp(-\alpha_0(r - r_{e1}))] \tag{5}$$

and

$$U_{Au-H}(r) = \gamma D_0 \exp(-2\alpha_H(r - r_{e2})). \tag{6}$$

The switch function of $S_2(r)$ has the form as in Equation (7)

$$S_2(r) = \begin{cases} 1 & \text{for } r \leq r_{on} \\ \dfrac{(r_{off}^2 - r^2)^2(r_{off}^2 + 2r^2 - 3r_{on}^2)}{(r_{off}^2 - r_{on}^2)^3} & \text{for } r_{on} < r < r_{off} \end{cases}, \tag{7}$$

The switch function of r_{on} and r_{off} has the start and end distances with the values of 7.0 and 11.0 Å, respectively.

3. RESULT AND DISCUSSION

3.1 The Fluidic Ejection

Figure 2 shows the fluidic nanojet for the different nozzle sizes and temperature values at the ejection time of 150000 femtosecond (fs). Figures 2(a)-(c) respectively show the pictures which the fluidic jets were ejected through 27.5, 30 and 40 Å diameter nozzles at a temperature value of 310 K under the same value of pressing force of 9.0×10^{-10} N. Figures 2(d)-(e) respectively show the pictures which the jets were ejected through the 27.5 Å diameter nozzle at temperature values of 315 and 333 K under the same value of pressing force of 9.0×10^{-10} N.

The results show that almost fluidic molecule is ejected out of the ejection device through the nozzle to form up the jets on the nozzle's surface at 150000 fs under the same value of pressing force of 9.0×10^{-10} N. Meanwhile, the fluidic jets leave the nozzle plate to manufacture the nanodroplets for the 30 and 40-Å-diameter nozzles at the temperature value of 310 K as shown in Figures 2(b)-(c). Figures 2(d)-(e) also give similar result for the 27.5 Å diameter nozzle at the temperature values of 315 and 333 K. Contrarily, fluidic jet does not leave the nozzle's plate to establish the fluidic droplet for the 27.5 Å diameter nozzle at the temperature value of 310 K as the photo shown in Figure 2(a).

3.2 The Fluidic Nanodroplet Formation

3.2.1 Influence of the Nozzle Diameter to the Nanodroplet Formation

The fluidic ejection and nanodroplet formation under the influence of different nozzle sizes at the same magnitudes of temperature and pressing force is as shown in Table 2. The droplets were separated for the 30 and 40 Å nozzle sizes at the temperature value of 310 K under the pressing force value of 9.0×10^{-10} N. Contrarily, The droplet was not formed for the 27.5 Å nozzle size at the temperature value of 310 K under the same pressing force magnitude.

Table 2. Effect of the different nozzle size to the nanodroplet formation

Temperature (K)	Pressing force (N)	Nozzle diameter (Å)		
		27.5	30	40
310	9.0×10^{-10}	Not nanodroplet formation	Nanodroplet formation	Nanodroplet formation

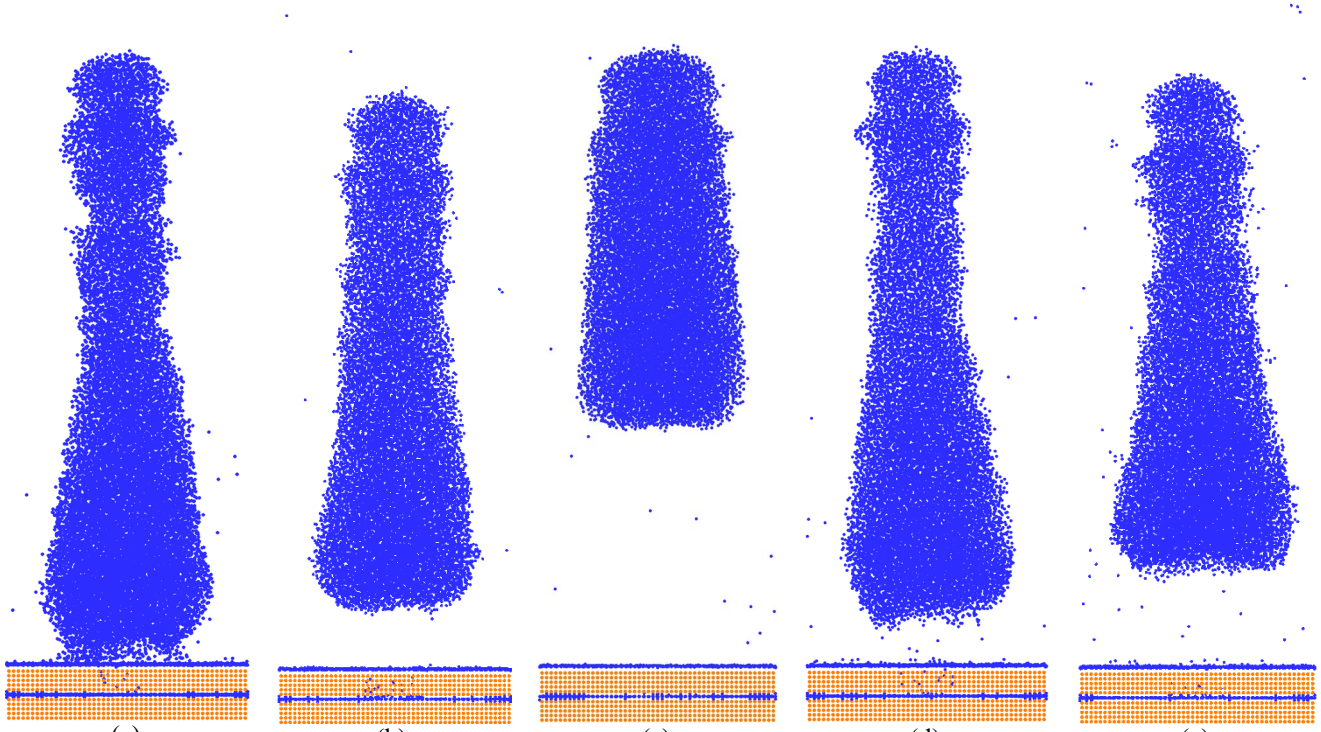

Figure 2. Photos of the fluidic nanojet at 150000 fs: (a)-(c) 27.5, 30 and 40 Å diameter nozzles and temperature of 310 K; (d)-(e) 27.5 Å diameter nozzles and temperature of 315 and 333 K

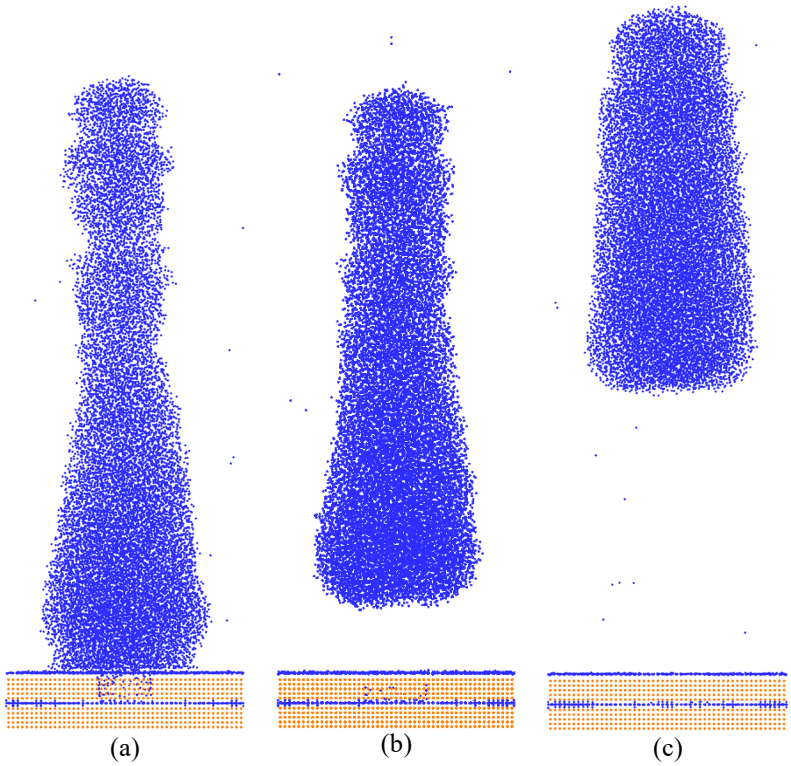

Figure 3. Photos of the fluidic jet at 200000 fs under 310 K temperature value and pressing force magnitude of 9.0×10^{-10} N. (a) 27.5 Å diameter nozzle; (b) 30 Å diameter nozzle; (c) 40 Å diameter nozzle

The pictures of the fluidic nanojet for the various nozzle sizes under the 310 K temperature and the pressing force of 9.0×10^{-10} N at 200000 fs are shown in Figure 3. In comparison between the photos of Figures 3(a)-(c) with the photos of Figures 2(a)-(c), we can see that the fluidic jets does not only separate out from the nozzle's surface but also continue to go up for the 30 and 40-Å-diameter nozzles as shown in Figures 3(b)-(c). However, the fluidic jet after reaching to the highest position at 150000 fs as shown in Figure 2(a) which moves down for the 27.5 Å diameter nozzle at the 310 K temperature value and pressing force magnitude of 9.0×10^{-10} N as shown in Figure 3(a). For a smaller nozzle size, the attraction force and cohesion

among the fluidic molecules are the main reasons which pull the liquid jet downward. That is the evidence for the fluidic nanodroplet formation under the influence of the nozzle size.

The fluidic molecular densities inside the ejection device for the 310 K temperature value and the 13.75, 15 and 20 Å radius nozzles are presented as in Figure 4. When the pressing force impacts on the fluidic molecules, the density magnitude has not much change in the ejection process for the 310 K temperature value and the 15 and 20 Å radius nozzles. Besides, this density rapidly increases from the beginning value of 0.378 to average value of 0.748 g/cm^3 for the 310 K temperature value and the 13.75 Å radius nozzle. However, this density is reduced back the initial value of 0.378 g/cm^3 after the ejection time of 110000 fs to the end of the ejection process. The high density causes many interactions among fluidic molecules inside the ejection device for the smaller nozzle size under the same magnitudes of temperature and pressing force. This also explains why the nozzle size has the effect to manufacture of the nanodroplets.

Figure 5 presents the distances from the average location of fluidic nanojet high to the nozzle's surface for the 310-K-temperature value and the 13.75, 15 and 20 Å radius nozzles. The average high of jet increases in Z direction from the initial ejection time to the ejection time of 140000 fs. These values continue to increase for the 15 and 20 Å radius nozzles. Meanwhile, the average distance of jet reduces down in *Z* direction after reaching to the high value of 140 Å for the 13.75 Å radius nozzle. This is an evidence for the effect of the nozzle size to manufacture the fluidic nanodroplet. The above evidences demonstrate and explain for the influence of nozzle size to the formation of liquid nanodroplet under the same magnitudes of temperature and pressing force.

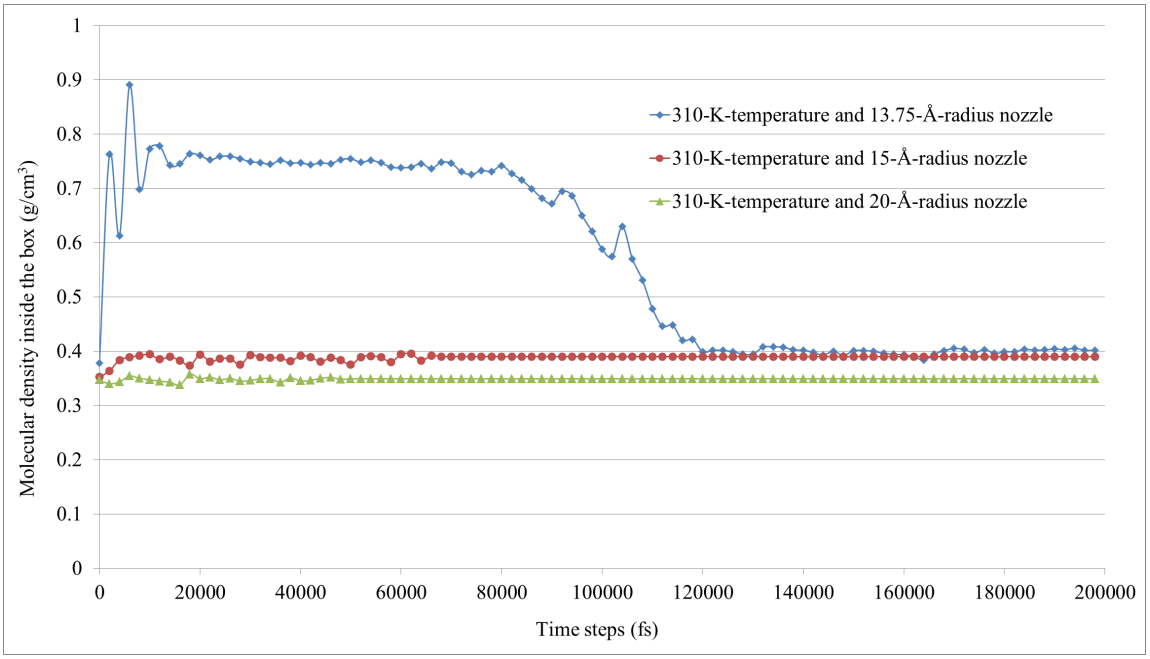

Figure 4. Fluidic molecular density inside the ejection device at each 2000 fs

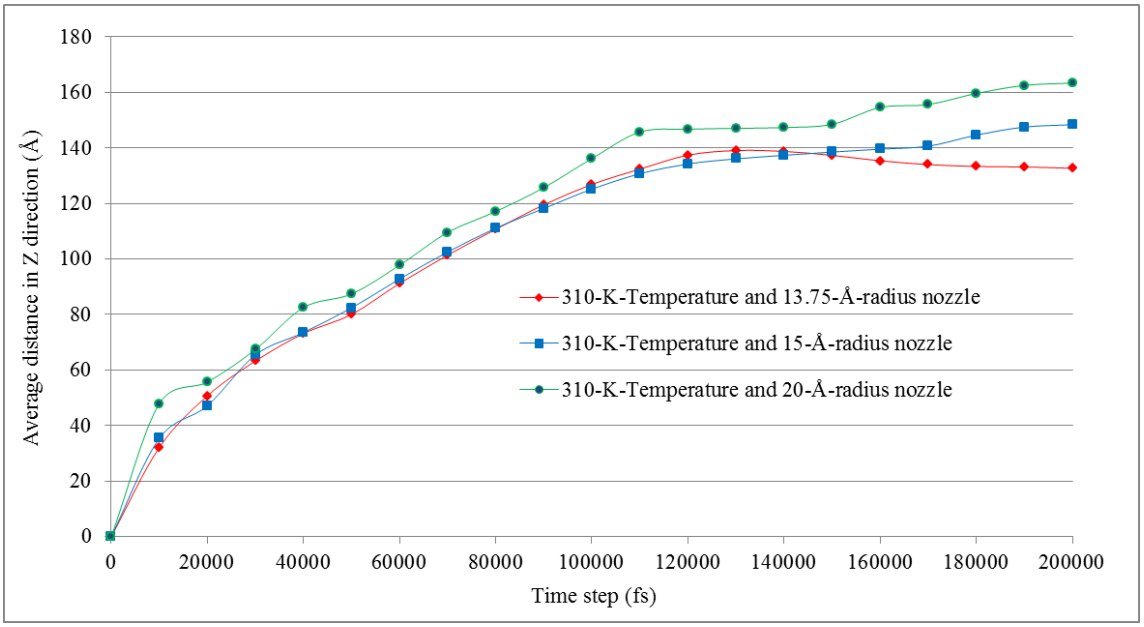

Figure 5. Distance from the average high of fluidic jet to the nozzle's surface in *Z* direction

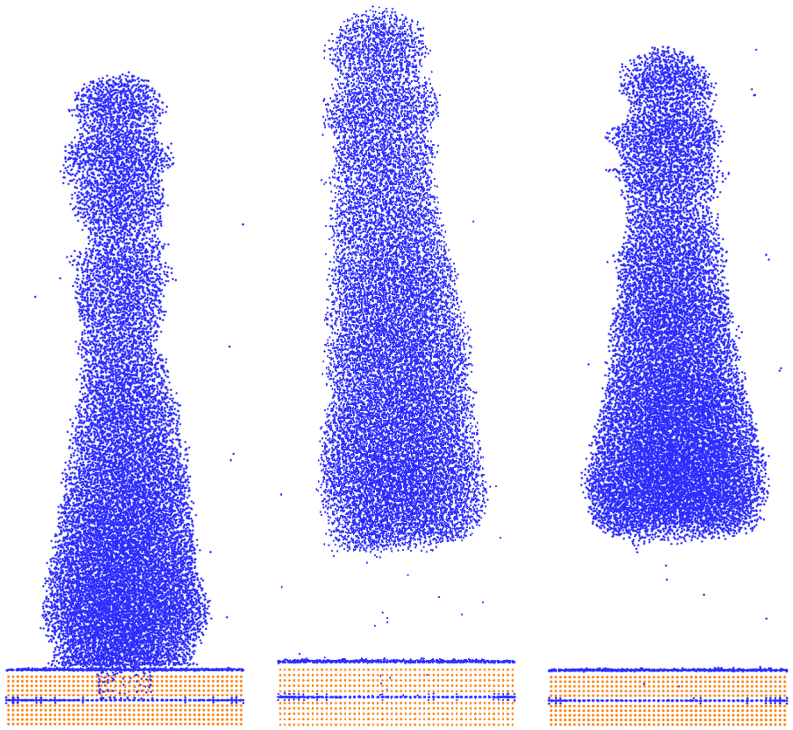

Figure 6. Photos of the nanojet at 200000 fs with 27.5 Å diameter nozzle and pressing force of 9.0×10^{-10} N. (a) 310 K temperature; (b) 315 K temperature; (c) 333 K temperature

3.2.2 Influence of the Temperature Value to the Fluidic Nanodroplet Formation

As results are shown in Table 3, at the same condition of 27.5 Å nozzle size and pressing force of 9.0×10^{-10} N, the fluidic nanodroplet is not formation for the temperature value of 310 K. However, the droplets are formed for the temperature values which are greater than or equal to 315 K when the fluidic jets were separated out from the nozzle's surface.

Table 3. Effect of the temperature magnitude to the nanodroplet formation

Nozzle diameter (Å)	Pressing force (N)	Temperature (K)		
		310	315	333
27.5	9.0×10^{-10}	Not nanodroplet formation	Nanodroplet formation	Nanodroplet formation

Figure 6 shows the photos of the fluidic nanojet which was ejected through the same nozzle diameter of 27.5 Å at pressing force of 9.0×10^{-10} N and the various temperature magnitudes of 310, 315 and 333 K at 200000 fs. In comparison between the photos of Figure 2(a), (d) and (e) with the photos of Figures 6(a)-(c), the results show that the fluidic nanodroplets were formed after separating out from the nozzle's surface to continue going up for the temperature values of 315 and 333 K. Besides, the fluidic jet goes down for the case of 27.5 Å diameter nozzle and 310 K temperature at 200000 fs as shown in Figure 6(a). This jet reaches to the highest position at the ejection time of 150000 fs as shown in Figure 2(a) under same value of the pressing force of 9.0×10^{-10} N.

Figure 7 shows the fluidic molecular density inside the ejection device for the 13.75 Å radius nozzle at temperature magnitudes of 310, 315 and 333 K under the same value of pressing force of 9.0×10^{-10} N. The density magnitude rapidly increases from the initial value of 0.378 g/cm^3 to average value of 0.751 g/cm^3 for the case of 13.75 Å radius nozzle at 310 K temperature. The density magnitude is smaller than of 0.751 g/cm^3 for the case of 13.75 Å radius nozzle at 315 K temperature. These densities were reduced back to near the initial value of 0.378 g/cm^3 after the ejection time of 110000 fs. Besides, the density magnitude increases and change in a narrow range at beginning stage. Then, this value rapidly reduces to value of 0.183 g/cm^3 after the ejection time of 80000 fs for the 13.75 Å radius nozzle at the 333 K temperature. The lower density magnitude inside the ejection device is the cause which has a little affection to the reduction of the molecular ejection velocity. Therefore, the fluidic nanodroplet is more easy formation for greater temperature magnitude.

Figure 8 shows the distances from the average positions of fluidic jet high to the nozzle's surface in Z direction for the 13.75 Å radius nozzles at the 310, 315 and 333 K temperature values. These values regularly increase from the initial time to the end of ejection process for the 13.75Å-radius nozzle at the temperature values of 315 and 333 K. However, this value is reduced down after the ejection time of 140000 fs for the case of the 13.75 Å radius nozzle and the 310 K temperature value. This is an evidence for the effect of the temperature magnitude to the formation of fluidic nanodroplet. These evidences explain why the temperature magnitude has effects to the fluidic jet breakdown for manufacturing the nanodroplets under the same conditions of pressing force and nozzle size.

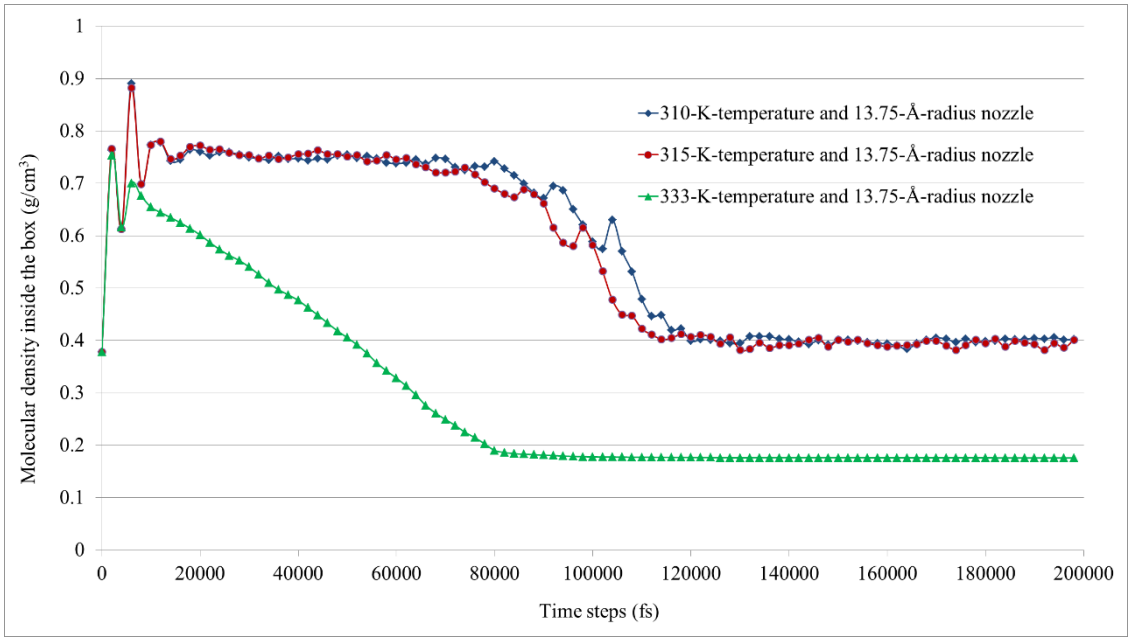

Figure 7. Fluidic molecular density inside the ejection device at each 2000 fs

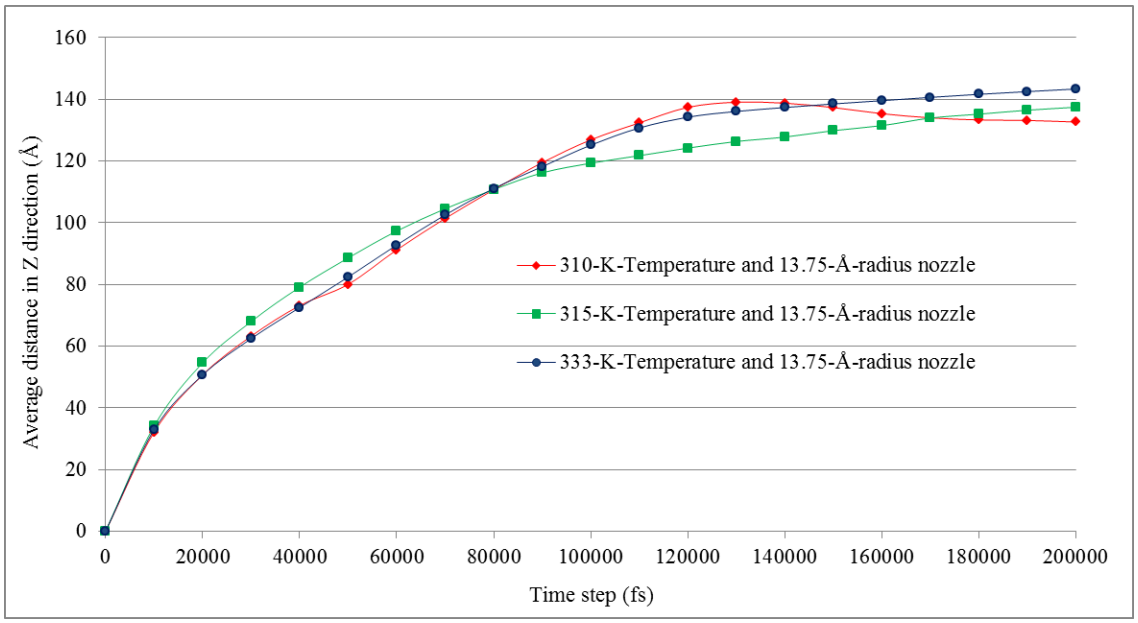

Figure 8. Distance from the average high of fluidic jet to the nozzle's surface in *Z* direction

4. CONCLUSION

The fluidic ejection and nanodroplet formation is studied by using the molecular dynamics simulation method. Based on the simulation results, the following conclusions were drawn:

- The fluidic molecules are ejected out through the nozzle hole to form up the jets on the nozzle's surface for the cases of 27.5, 30 and 40 Å nozzle diameters at 310, 315 and 333 K temperature values under the same magnitude of the pushing force of 9.0×10^{-10} N.
- However, for the case of 27.5 Å nozzle diameter at 310 K temperature value, the fluidic jet after forming up and reaching to the highest position at 150000 fs which does not leave from the nozzle's surface to get the fluidic nanodroplets. That is due to the attractive force between the jet's fluidic molecules with the nozzle plate's metallic atoms is greater than the inner connective force among the jet's fluidic molecules. Therefore, the fluidic jet cannot separate out from the nozzle to form up the droplet.
- Contrarily, when increasing the magnitude of either nozzle diameter or temperature which the fluidic jet is leaved out from the nozzle's surface to form the droplets. This can be explained by the time and fluidic ejection though the nozzle are more fast and easy for these cases. Therefore, the energy and velocity of the fluidic molecules after forming jet are still great that can win the attractive force between the jet's molecules with the nozzle plate's atoms to form up the fluidic droplets. That means the nozzle diameter and temperature have the influences to the formation of the fluidic nanodroplet.

ACKNOWLEDGMENT

This research was partially supported by Department of Sciences and Technology, Hanoi University of Industry, Viet Nam.

REFERENCES

[1] H. Jiang and H. Tan, One dimensional model for droplet ejection process in inkjet devices, *Fluids*, 3(2), 2018, 28.
[2] D. Osmanovic and Y. Rabin, Chemically active nanodroplets in a multi-component fluid, *Soft Matter*, 15, 2019, 5965-5972.
[3] C. D. Modak, A. Kumar, A. Tripathy and P. Sen, Drop impact printing, *Nature Communications*, 11, 2020, 4327.
[4] H.-H. Lee, K.-S. Chou and K.-C. Huang, Inkjet printing of nanosized silver colloids, *Nanotechnology*, 16(10), 2005, 2436-2441.
[5] L. Kondic, J. A. Diez, P. D. Rack, Y. Guan and J. D. Fowlkes, Nanoparticle assembly via the dewetting of patterned thin metal lines: Understanding the instability mechanisms, *Physics Review E*, *Statistical, Nonlinear and Soft Matter Physics*, 79(2), 2009, 026302.
[6] A. Tiwari and J. Abraham, Dissipative particle dynamics simulations of liquid nanojet breakup, *Microfluidics and Nanofluidics*, 4, 2008, 227-235.
[7] C.-F. Dai and R.-Y. Chang, Molecular dynamics simulation of formation and control of nanodroplets in piezoelectric nanoejection systems, *Molecular Simulation*, 36(11), 2010, 847-855.
[8] X. Zhang, Z. Lu, H. Tan, L. Bao, Y. He, C. San and D. Lohse, Formation of surface nanodroplets under controlled flow conditions, *The Proceedings of the National Academy of Sciences (PNAS)*, 112(30), 2015, 9253-9257.
[9] J. Meng, J. B. You and X. Zhang, Viscosity-mediated growth and coalescence of surface nanodroplets, *The Journal of Physical Chemistr*y, 124(23), 2020, 12476–12484.
[10] J. Qian, G. F. Arends and X. Zhang, Surface nanodroplets: Formation, dissolution, and applications, *Langmuir*, 35 (39), 2019, 12583-12596.
[11] M. Moseler and U. Landman, Formation, stability, and breakup of nanojets, *Science*, 289(5482), 2000, 1165-1170.
[12] C. P. Steinert, I. Goutier, O. Gutmann, H. Sandmaier, M. Daub, B. de Heij and R. Zengerle, A highly parallel picoliter dispenser with an integrated, novel capillary channel structure, *Sensor and Actuators A: Physical*, 116, 2004, 171-177.
[13] M. Ibrahim, T. Otsubo, H. Narahara, H. Koresawa and H. Suzuki, Inkjet printing resolution study for multi-material rapid, *JSME International Journal Series C Mechanical Systems, Machine Elements and Manufacturing*, 49(2), 2006, 353-360.
[14] A. Dalili, S. Chandra, J. Mostaghimi, H. T. Charles Fan and J. C. Simmer, Formation of liquid sheets by deposition of droplets on a surface, *Journal of Colloid and Interface Science*, 418, 2014, 292–299.
[15] J.-W. Lin and S.-X. Chu, Molecular dynamics simulations of nanoscale water jet, *Proceedings of ASME First International Conference on Micro/Nanoscale Heat Transfer*, Taiwan, 2008, 519-524.
[16] Y. Li, J. Xu and D. Li, Molecular dynamics simulation of nanoscale liquid flows, *Microfluidics and Nanofluidics*, 9, 2010, 1011-1031.
[17] N. Gopan and S. P. Sathian, The role of thermal fluctuations on the formation and stability of nano-scale drops, *Colloids and Surfaces A: Physicochemical and Engineering Aspects*, 432, 2013, 19-28.
[18] J.-W. Lin, Studying on water nanojet ejection and the wetting phenomena on the nozzle surface, *Microfluidics and Nanofluidics*, 13, 2012, 37-48.
[19] N. Gopan and S. P. Sathian, A langevin dynamics study of nanojets, *Journal of Molecular Liquids*, 200(B), 2014, 246-258.
[20] T. Fu, Y. Wu, Y. Ma and H. Z. Li, Droplet formation and breakup dynamics in microfluidic flow-focusing devices: From dripping to jetting, *Chemical Engineering Science*, 84, 2012, 207-217.
[21] C.-T. Lin, J.-K. Kuo and T.-H. Yen, Three-dimensional molecular dynamics study of aperture shape effect on nanojet ejection, *Journal of the Chinese Institute of Engineers*, 34, 2011, 1001-1011.
[22] J. Eggers, Dynamics of liquid nanojets, *Physics Review Letter*, 89(8), 2002, 084502.
[23] T.-H. Fang, W.-J. Chang and S.-L. Lin, Effects of temperature and velocity of droplet ejection process of simulated nanojets onto a moving plate's surface, *Applied Surface Science*, 253(3), 2006, 1649-1654.
[24] S. Aphinyan, E. Y. M. Ang, J. Yeo, T. Y. Ng, R. Lin, Z. Liu and K. R. Geethalakshmi, Many-body dissipative particle dynamics simulations of nanodroplet formation in 3D nano-inkjet printing, *Modelling and Simulation in Materials Science and Engineering*, 27(5), 2019, 055005.
[25] K.-T. Chang and C.-I. Weng, An investigation into the structure of aqueous NaCl electrolyte solutions under magnetic fields, *Computational Material Science*, 43(4), 2008, 1048-1055.
[26] B. Beulen, J. de Jong, H. Reinten, M. van den Berg, H. Wijshoff and R. van Dongen, Flows on the nozzle plate of an inkjet print head, *Experiments in Fluids*, 42, 2007, 217-224.
[27] A. Asai, Three-dimensional calculation of bubble growth and drop ejection in a bubble jet printer, *Journal of Fluids Engineering*, 114(4), 1992, 638-641.
[28] V. Q. Nguyen and J.-W. Lin, Investigation of temperature effects on nanoscale water droplet separation from a nozzle plate and impingement onto a fixed solid plate, S*IMULATION*, 92(10), 2016, 945-953.
[29] M. Levitt, M. Hirshberg, R. Sharon, K. E. Laidig and V. Dagget, Calibration and testing of a water model for simulation of the molecular dynamics of proteins and nucleic acids in solution, *The Journal of Physical Chemistry B*, 101(25), 1997, 5051-5061.